

Unperturbed Expression Bias of Imprinted Genes in Schizophrenics

Attila Gulyás-Kovács*, Ifat Keydar*, ..., Andrew Chess

Mount Sinai School of Medicine

Abstract

We present a genome-wide analysis of human genomic imprinting based on RNA-seq measurements of parental bias in allele-specific expression in the dorsolateral prefrontal cortex. We find that the fraction of imprinted human genes is consistent with lower ($\approx 0.5\%$) as opposed to higher ($\approx 5\%$) estimates in mice. Our analysis reveals that age up or down-regulates allelic bias of some, but not all, imprinted genes in adulthood and that allelic bias depends also on genetic variation. These results support the hypothesized role of imprinted genes in social interactions, which dynamically change in the life course and depend on neuropsychological function.

1 Introduction

Genomic imprinting, leading to repression of either the maternal or paternal allele, has reached its highest prevalence in humans and other placental organisms [17]. In line with this, well-known physiological functions of imprinted genes include embryonic and placental development, body growth, suckling, and maternal behavior [16, 15]. Genomic imprinting requires the placement of different epigenetic marks, such as DNA methylation, at the respective alleles residing on the chromosomes originating from the mother or father [16]. Indeed, imprinted genes typically reside in clusters spanning hundreds of kilobases and allele-specific differential epigenetic marks are found near specific genes as well as in shared regulatory elements called imprinting control regions. For non-imprinted genes expression is balanced such that the two alleles are roughly equally expressed. By contrast, for imprinted genes epigenetic marks lead to substantial degrees of imbalance in the expression level of the two alleles. We refer to the degree of expression imbalance as *allelic bias*; at its maximum expression is completely monoallelic.

Why natural selection favors allelic bias for imprinted genes remains debated [20, 12, 11] but the most mature of all theories, kinship or conflict theory [20], provides a flexible framework for interpreting past studies on imprinted genes and formulating hypotheses and predictions regarding their detailed regulation and physiological function. The theory assumes that all imprinted genes contribute to inter-individual interactions in a highly dose-dependent fashion, and explains allelic bias with the conflicting interests of paternal and maternal genes, which arise from sexual asymmetries in those interactions [20]. A well-known asymmetry is the disproportionate role of mothers in nurturing offspring in Placentalia. Kinship theory thus explains why overexpression disorders of paternally or maternally biased genes in children abnormally promote or inhibit, respectively, their growth [16, 15].

Since different inter-individual interactions take place in various developmental stages and are mediated by various organs, kinship theory explains the non-uniform pattern of “imprintedness” and allelic bias over various ages [3] and tissue types, which is seen for several imprinted genes [16, 15]. For other genes such patterns await discovery. The theory quantitatively predicts relaxation of allelic conflict with age [19] and so raises the hypothesis that change in allelic bias is linked to aging. A study on newborn and young adult mice partially supports that hypothesis [14] but experimental evidence from humans, including older individuals, is missing.

In the framework of kinship theory the question of aging is closely tied to the roles of imprinted genes in social interactions and in the underlying psychiatric functions [19, 20], whose importance has been increasing in human evolution. Indeed, most human imprinted gene syndromes are characterized by not only growth disorder but also mental retardation and psychiatric dysfunction [16, 15]. More precisely, paternally and maternally biased genes are suggested to play antagonistic roles not only in growth but also in psychiatric functions [5], since overexpression of the former is associated with autistic while that of the latter with psychotic spectrum disorders. For example, maternally derived microduplications at 15q11-q13 may not only cause the Prader-Willi syndrome [15]—whose symptoms include obesity—but also highly penetrant for schizophrenia [9, 18], which is perhaps the most devastating psychotic spectrum disorder.

Recently the CommonMind Consortium produced and shared¹ genome-wide data sets on genotype and gene expression in the dorsolateral prefrontal cortex (DLPFC) of hundreds of schizophrenic and control individuals, and identified some 650 differentially expressed genes [7]. Our present work extends that analysis with a focus on allele-specific expression across the genome, allowing us to determine allelic bias for each gene. Based on that, we find that $\approx 0.6\%$ of all genes are imprinted in the human DLPFC, the majority of which had been reported to be imprinted in the context of one or another tissue and/or species. We find a number of genes with allele specific expression residing near clusters of known imprinted genes. Furthermore, our data suggest that for several imprinted genes the variation of allelic bias across individuals is explained by differences in ancestry and age in a manner that depends on the gene.

2 Methods

2.1 Defining the read count ratio to quantify allelic bias

We quantified allelic bias based on RNA-seq reads using a statistic called *read count ratio* S , whose definition we based on the total read count T and the *higher read count* H , i.e. the count of reads carrying only either the reference or the alternative SNP variant, whichever is higher. The definition is

$$S_{ig} = \frac{H_{ig}}{T_{ig}} = \frac{\sum_s H_s}{\sum_s T_s}, \quad (1)$$

where i identifies an individual, g a gene, and the summation runs over all SNPs s for which gene g is heterozygous in individual i (Fig. 1). Note that if B_{ig} is the count of reads that map to the b_{ig} allele (defined as above) and if we make the same distributional assumption as above, namely that $B_{ig} \sim \text{Binom}(p_{ig}, T_{ig})$, then $\Pr(H_{ig} = B_{ig} | p_{ig})$, the probability of correctly assigning the reads with the higher count to the allele towards which expression is biased, tends to 1 as $p_{ig} \rightarrow 1$. We took advantage of this theoretical result in that we subjected only those genes to statistical inference,

¹www.commonmind.org

whose read count ratio was found to be high and, therefore, whose p_{ig} is expected to be high as well.

Fig. 1 illustrates the calculation of S_{ig} for the combination of two hypothetical genes, g_1, g_2 , and two individuals, i_1, i_2 . It also shows an example for the less likely event that the lower rather than the higher read count corresponds to the SNP variant tagging the higher expressed allele (see SNP s_3 in gene g_1 in individual i_2).

Before we carried out our read count ratio-based analyses, however, we cleaned our RNA-seq data by quality-filtering and by improving the accuracy of SNP calling with the use of DNA SNP array data and imputation. In the following subsections of Methods we describe the data, these procedures, as well as our regression models in detail.

2.2 Data

2.2.1 Brain samples, RNA-seq

Human RNA samples were collected from the dorsolateral prefrontal cortex of the CommonMind consortium from a total of 579 individuals after quality control. Subjects included 267 control individuals, as well as 258 with schizophrenia (SCZ) and 54 with affective spectrum disorder (AFF). RNA-seq library preparation uses Ribo-Zero (which selects against ribosomal RNA) to prepare the RNA, followed by Illumina paired end library generation. RNA-seq was performed on Illumina HiSeq 2000.

2.2.2 Mapping, SNP calling and filtering

We mapped 100bp, paired-end RNA-seq reads (≈ 50 million reads per sample) using Tophat to Ensembl gene transcripts of the human genome (hg19; February, 2009) with default parameters and 6 mismatches allowed per pair (200 bp total). We required both reads in a pair to be successfully mapped and we removed reads that mapped to > 1 genomic locus. Then, we removed PCR replicates using the Samtools rmdup utility; around one third of the reads mapped (which is expected, given the parameters we used and the known high repeat content of the human genome). We used Cufflinks to determine gene expression of Ensembl genes, using default parameters. Using the BCFtools utility of Samtools, we called SNPs (SNVs only, no indels). Then, we invoked a quality filter requiring a Phred score > 20 (corresponding to a probability for an incorrect SNP call < 0.01).

We annotated known SNPs using dbSNP (dbSNP 138, October 2013). Considering all 579 samples, we find 936,193 SNPs in total, 563,427 (60%) of which are novel. Further filtering of this SNP list removed the novel SNPs and removed SNPs that either did not match the alleles reported in dbSNP or had more than 2 alleles in dbSNP. We also removed SNPs without at least 10 mapped reads in at least one sample. Read depth was measured using the Samtools Pileup utility. After these filters were applied, 364,509 SNPs remained in 22,254 genes. These filters enabled use of data with low coverage. For the 579 samples there were 203 million reads overlapping one of the 364,509 SNPs defined above. Of those 158 million (78%) had genotype data available from either SNP array or imputation.

2.2.3 Genotyping and calibration of imputed SNPs

DNA samples were genotyped using the Illumina Infinium SNP array. We used PLINK with default parameters to impute genotypes for SNPs not present on the Infinium SNP array using 1000 genomes data. We calibrated the imputation parameters to find a reasonable balance between the number of genes assessable for allelic bias and the number false positive calls since the latter can arise if a SNP is incorrectly called heterozygous.

We first examined how many SNPs were heterozygous in DNA calls and had a discordant RNA call (i.e. homozygous SNP call from RNA-seq) using different imputation parameters. Known imprinted genes were excluded. We examined RNA-seq reads overlapping array-called heterozygous SNPs which we assigned a heterozygosity score L_{het} of 1, separately from RNA seq data overlapping imputed heterozygous SNPs, where the L_{het} score could range from 0 to 1. After testing different thresholds we selected an L_{het} cutoff of 0.95 (i.e. imputation confidence level of 95%), and a minimal coverage of 7 reads per SNP. With these parameters, the discordance rate (monoallelic RNA genotype in the context of a heterozygous DNA genotype) was 0.71% for array-called SNPs and 3.2% for imputed SNPs.

The higher rate of discordance for the imputed SNPs is due to imputation error. These were taken into account in two ways. First, we considered all imputed SNPs for a gene g and individual i jointly. Second, we excluded any individual, for which one or more SNPs supported biallelic expression.

2.2.4 Quality filtering

Two kind of data filters were applied sequentially: (1) a *read count-based* and (2) an *individual-based*. The read count-based filter removes any such pair (i, g) of individual i and genes g for which the total read count $T_{ig} < t_{\text{rc}}$, where the read count threshold t_{rc} was set to 15. The individual-based filter removes any genes g (across all individuals) if read count data involving g are available for less than t_{ind} number of individuals, set to 25. These final filtering procedures decreased the number of genes in the data from 15584 to $n = 5307$.

2.3 Test for nearly unbiased expression

This test was defined by the criterion

$$S_{ig} \leq 0.6 \text{ and } \text{UCL}_{ig} \leq 0.7, \quad (2)$$

where the 95% upper confidence limit UCL_{ig} for the expected read count ratio p_{ig} was calculated based on the assumption that the higher read count $H_{ig} = S_{ig}T_{ig} \sim \text{Binom}(p_{ig}, T_{ig})$, on the fact that binomial random variables are asymptotically (as $T_{ig} \rightarrow \infty$) normal with $\text{var}(H_{ig}) = T_{ig}p_{ig}(1-p_{ig})$, and on the equalities $\text{var}(S_{ig}) = \text{var}(H_{ig}/T_{ig}) = \text{var}(H_{ig})/T_{ig}^2$. Therefore

$$\text{UCL}_{ig} = S_{ig} + z_{0.975} \sqrt{\frac{S_{ig}(1-S_{ig})}{T_{ig}}}, \quad (3)$$

where z_p is the p quantile of the standard normal distribution.

2.4 Regression analysis

2.4.1 Mixed and fixed models

We modeled the dependence of read count ratio of imprinted genes on biological and technical explanatory variables (Table S1) using mixed and fixed generalized linear models (GLMs).

GLMs in general describe a conditional distribution of a response variable y given a linear predictor η such that the distribution is from the exponential family and that $E(y|\eta) = g^{-1}(\eta)$, where g is some link function. In the present context the response y is the observed read count ratio that is possibly transformed to improve the model’s fit to the data. We performed fitting with the lme4 and stats R packages and tested several combinations of transformations, link functions, and error distributions (Table S2). For inference we used the best fitting combination (unlm.Q, Table S2) as assessed by the normality (Fig. S2) and homoscedasticity (Fig. S3) of residuals as well as by monitoring convergence.

In mixed GLMs the linear predictor $\eta = X\beta + Zb$ and in fixed GLMs $\eta = X\beta$, where X, Z are design matrices containing data on explanatory variables whereas β and b are fixed and random vectors of regression coefficients that mediate fixed and random effects, respectively (see Section 2.4.2 and Fig. S1 for details).

Besides the random effects term Zb the key difference between the mixed and fixed models in this study is that the former describes read count ratio *jointly* for all imprinted genes and the latter *separately* for each imprinted gene. An important consequence is that our mixed models are more powerful because they can utilize information shared by all genes. Therefore we preferred mixed models for final inference and used fixed models only to guide selection among possible mixed models (Section 2.4.3).

2.4.2 Formulation and interpretation of mixed models

Here we describe the detailed syntax and semantics of the normal linear mixed models combined with a quasi-log transformation Q of read count ratio as this combination was found to provide the best fit (Fig. S2, S3). We have data on 579 individuals and 30 imprinted genes and so the response vector is $y = (Q_{i_1g_1}, \dots, Q_{i_{579}g_1}, Q_{i_1g_2}, \dots, Q_{i_{579}g_2}, \dots, Q_{i_1g_{30}}, \dots, Q_{i_{579}g_{30}})$. The model in matrix notation is

$$y = X\beta + Zb + \varepsilon \quad (4)$$

$$\varepsilon_i \stackrel{\text{i.i.d.}}{\sim} \mathcal{N}(0, \sigma^2), \quad i = 1, \dots, mn \quad (5)$$

$$b \sim \mathcal{N}(0, \Omega_b), \quad (6)$$

where the size of the covariance matrix Ω_b depends on the number of terms with random effects (the columns of Z). Simply put: errors and random coefficients are all normally distributed.

To clarify the semantics of Eq. 4 let us consider a simple toy model with just a few terms in the linear predictor. But before expressing it in terms of Eq. 4 it is easier to cast it in the compact “R formalism” of the stats and lme4 packages of the R language as

$$y \sim \overbrace{1 + \text{Age}}^{\text{fixed effect}} + \underbrace{(1 + \text{Age} + \text{Ancestry.1} \mid \text{Gene})}_{k=1} + \underbrace{(1 \mid \text{Dx} : \text{Gene})}_{k=2}. \quad (7)$$

First note that the random effect term labeled with $k = 1$ can be expanded into $(1 | \text{Gene}) + (\text{Age} | \text{Gene}) + (\text{Ancestry.1} | \text{Gene})$. The ‘1’s mean intercept terms: one as a fixed effect and two as random effects. The first random intercept term $(1 | \text{Gene})$ expresses the gene-to-gene variability in read count ratio (compare panels in Fig. 4 and 5), in other words the random effect of the Gene variable. The second random intercept term $(1 | \text{Dx} : \text{Gene})$ corresponds to the interaction between psychiatric diagnosis Dx and Gene; it can be interpreted as the Gene specific effect of Dx or—equivalently—as Dx specific gene-to-gene variability. This term is not likely to be informative as Fig. 4 suggests little Gene specific effect of Dx.

We see that Age appears twice: first as a fixed slope effect on y and second as a Gene specific random slope effect, denoted as $(\text{Age} | \text{Gene})$. The random effect appears to be supported by Fig. 5 because the dependence of read count ratio on Age varies substantially among genes but the fixed effect is not supported because the negative dependence seen for several genes is balanced out by the positive dependence seen for others. The model includes another random slope effect: $(\text{Ancestry.1} | \text{Gene})$ with a similar interpretation as $(\text{Age} | \text{Gene})$ but lacks a fixed effect of Ancestry.1.

Now we are ready to write the toy model as an expanded special case of Eq. 4 as

$$y_i = \underbrace{\beta_0 + \text{Age}_i \beta_1}_{\text{fixed effects}} + \underbrace{b_0^{(1)} + \text{Age}_i b_1^{(1)} + \text{Ancestry.1}_i b_2^{(1)}}_{\text{Gene}_i} + \underbrace{b_0^{(2)}}_{\text{Dx}_i : \text{Gene}_i} + \varepsilon_i. \quad (8)$$

As in the earlier R formalism the terms of the linear predictor are grouped into fixed and random effects. Within the latter group we have two batches of terms indicated by the k superscripts on the random regression coefficients $b_j^{(k)}$. The first batch $\{b_0^{(1)}, b_1^{(1)}, b_2^{(1)}\}$ corresponds to $\{(1 | \text{Gene}), (\text{Age} | \text{Gene}), (\text{Ancestry.1} | \text{Gene})\}$ in Eq. 7, the second batch contains only $b_0^{(2)}$ corresponding to $(1 | \text{Dx} : \text{Gene})$.

Within the k th batch Eq. 8 contains only a single intercept coefficient $b_0^{(k)}$ and, if random slope terms are also present in the batch, only a single slope coefficient associated with the variable Age or Ancestry.1. This is because only a single level of the factor Gene or the composite factor Dx : Gene needs to be considered for the i th observation; these levels are denoted as Gene_i and $\text{Dx}_i : \text{Gene}_i$, respectively. Implicitly however, Eq. 8 contains the respective coefficients for all levels of these factors. For example, there are $n = 30$ intercept coefficients $b_j^{(1)}$ each of which corresponds to a given gene. So to generalize Eq. 8 we need J_k coefficients in the k th batch, where J_k is the product of the number of factor levels and one plus the number of random slope variables. This way we can provide the expansion of the general formula Eq. 4 using the semantics of the toy model (Eq. 7, 8) as

$$y_i = \underbrace{\sum_{j=0}^J x_{ij} \beta_j}_{\text{fixed effects}} + \underbrace{\sum_{k=1}^K \sum_{j=0}^{J_k} z_{ij}^{(k)} b_j^{(k)}}_{\text{random effects}} + \varepsilon_i. \quad (9)$$

2.4.3 Model fitting and selection

Eq. 9 describes a large set of mixed models that differ in one or more individual terms that constitute their linear predictor. From this set we aimed to select the best fitting model under the Akaike Information Criterion (AIC).

We used a heuristic search strategy in order to restrict the vast model space to a relatively small subset of plausible models. The search was started at a model whose relatively simple linear predictor was composed of terms using our prior results based on fixed effects models. The same results suggested a sequence in which further terms were progressively added to the model to test if they improve fit. Improvement was assessed by ΔAIC and the χ^2 -test on the degrees of freedom that correspond the evaluated term. If fit improved the term was added otherwise it was omitted. Next, further terms were tested. This iterative procedure lead to the following model.

$$\begin{aligned} Q \sim & \text{RIN} + (1 \mid \text{RNA_batch}) + (1 \mid \text{Institution}) + (1 \mid \text{Institution} : \text{Individual}) \\ & + (1 \mid \text{Gene} : \text{Institution}) + (1 \mid \text{Gender} : \text{Gene}) \\ & + (\text{Age} + \text{RIN} + \text{Ancestry.1} + \text{Ancestry.3} \mid \text{Gene}) \end{aligned}$$

We refer to this as the “best fitting model” even though it may represent only a local optimum in model space.

3 Results

3.1 Genome- and population-wide variation of allelic bias

A total of 5307 genes passed our filters designed to remove genes with scarce RNA-seq data reflecting low expression and/or low coverage of RNA-seq. Examining these genes, we performed exploratory statistical analysis based on the read count ratio statistic S_{ig} , whose results (below) we interpreted in terms of the variation of allelic bias both across genes g and across individuals i . Note that our later analyses (Section 3.3 and below) used information not only in S_{ig} but also in the total read count as well as in data beyond RNA-seq.

Fig. 2 presents the conditional empirical distribution of $S_{.g}$ given each gene g . Each of the three plots of the upper half show in a distinct representation the same empirical distributions based on data for three genes. The main panels of the lower half present, in the most compact representation, the distributions based on all data (5307 genes). Two of the three genes in the upper half, PEG10 and ZNF331, are *known imprinted* genes in the sense that they had previously been found imprinted in the context of some developmental stage, species, and tissue type other than the adult human DLPCF. The third, AFAP1, has not been reported to be imprinted in any context. For all three genes $S_{.g}$ varies considerably within its theoretical range $[\frac{1}{2}, 1]$. This suggests variation of allelic bias across study individuals, although some component of the variation of $S_{.g}$ must originate from technical sources.

To identify imprinted genes based on the read count ratio we defined the score of each gene g as the location statistic $1 - \text{ECDF}_g(0.9)$, which is the fraction of individuals i for whom $S_{ig} > 0.9$. We ranked all 5307 genes according to their score shown in the side plots of the lower half of Fig. 2 as gray filled circles. Larger green circles mark the three genes mentioned above. The heat map of empirical distribution of $S_{.g}$ of ranked genes (Fig. 2, lower left) suggests that the top 50 genes, which constitute $\approx 1\%$ of all genes in our analysis, are qualitatively different from the bottom $\approx 99\%$ suggesting that most of them are imprinted. Consistent with this, the top-scoring genes tended to cluster around genomic locations that had been previously described as imprinted gene clusters (Fig. S4).

3.2 Imprinted genes in the adult DLPC cortex

The set of top scoring 50 genes is highly enriched in known imprinted genes, marked by blue in Fig. 3 and in *nearby candidate* genes (green) defined as being within 1Mb of a known imprinted gene. Within the top 50, we find 29 such genes; 21 known imprinted genes and eight nearby candidates.

The remaining 21 genes in the top 50 are separated by > 1 Mb from some known imprinted gene (termed *distant candidates*, red in Fig. 3). Upon further examination these distant candidate genes are overwhelmingly likely not imprinted. The primary reason for this conclusion is that we performed a test to see if there is reference allele bias for all candidate genes. For any gene (known imprinted, or candidate) the expectation is that when some allelic bias is detected, that should equally favor the reference or non-reference allele since for a given individual who is heterozygous at a given SNP in the genome it is reasonable to assume that the chances are equal that the mother or that the father has the reference allele. Most known imprinted genes and the nearby candidates display a reference/non-reference distribution consistent with a binomial distribution with a probability of 0.5 for both the reference and non-reference alleles. However, and in sharp distinction, most distant candidates have distributions of reference/non-reference that are not consistent with equal probabilities (see genes marked with “X” in Fig. 3). Indeed, for most of them the distribution is shifted towards the reference allele strongly suggesting that mistaken genotyping, imputation or a mapping issue led to the presence of these red genes in the list of the top 50 genes. One could argue that we should have left these genes out of Fig. 3, but we thought it was important to show them and to indicate the reasons they are set aside. Note also, that we also tested the hypothesis for each gene g and individual i that allelic expression is (nearly) unbiased (Eq. 2). The fraction of individuals for which the test was *not* rejected tends to be much higher for the “red” genes in the top 50 (black bars in Fig. 3).

While the shifted distribution of reference/non-reference alleles leads us to discount the possibility of imprinting, random monoallelic expression is still a distinct possibility for these candidates as our studies of random monoallelic expression in mice suggested that a substantial fraction (40–80%) of random monoallelically-expressed genes had a very strong bias towards monoallelic expression of one of the two alleles [22]. Moreover, it is worth noting that three of these candidates are from the major histocompatibility locus (HLA), which is notable for extensive polymorphism and difficulties with allelic identification. For these three genes we also analyzed them more thoroughly with HLA-specific methods for determining haplotype based on RNA-seq [1] and genotype data [21]. The high observed read count ratios for HLA genes appear to be driven by eQTL-like effects, not by random monoallelic expression nor by imprinting (manuscript in preparation). Examining all the assessable known imprinted genes, we find that $\frac{1}{3}$ rd of them have a low gene score. This suggests that these genes do not display imprinted expression in the human adult DLPC, consistent with many reports in the literature indicating that known imprinted genes are often imprinted in some but not all tissues.

In subsequent analysis (below) we also consider UBE3A as demonstrating allelic bias consistent with imprinting in the context of human adult DLPC as evidenced by Fig. S5 even though its rank falls outside of the top 50. Thus, we have thirty genes we consider imprinted in the adult DLPC.

3.3 Allelic bias of imprinted genes and schizophrenia

Given that our sample is comprised of neurotypic individuals (Control) as well as individuals with schizophrenia (SCZ) and with affective spectrum disorder (AFF), we explored whether there

is any association between diagnosis and allelic bias of imprinted genes. Fig. 4 compares read count ratio distribution among control, SCZ and AFF for the 30 imprinted genes and suggests there are no differences among the three groups.

To further explore the data, we performed statistical inference using mixed effects models. With this procedure we quantified the extent the read count ratio is dependent on diagnosis and other explanatory variables. These included biological variables namely Age, the first five principal components of ancestry (Ancestry.1,...,Ancestry.5), Gender and also technical variables such as RIN, the RNA integrity number (see Table S1 for complete list). Our mixed regression models describe the dependence of read count ratio on some or all of the explanatory variables simultaneously, which allows the dissection of various biological and technical sources of variation. Another benefit of the mixed modeling framework is its power with respect to global, not gene-specific, parameters because it makes use of information that is only available when all thirty genes are considered simultaneously; still, it allows the prediction gene-specific regression coefficients (Fig. S1 right). These benefits however hinge on the goodness of model fit to the data. Therefore, we fitted many alternative mixed models, selected the best-fitting one using the Akaike Information Criterion (AIC) and confirmed the goodness of fit with diagnostic plots (Section 2.4.3, Fig. S2, S3).

Based on the selected, best fitting, model we formally tested whether read count ratio depends on various predictor terms that represent either the main effect of some biological variable or the interaction between two variables (Table 1). For example, given prior observations as well as the empirical distribution of data in Figures 4 and 5, one would expect the model-based test should detect gene-to-gene variability of read count ratio. Indeed that variability—more precisely the random main effect ($1 \mid \text{Gene}$) of the Gene variable—is strongly supported by the test with a ΔAIC of -127 and a p-value of $< 10^{-27}$ (Table 1).

Returning to our main question the model-based test did not support any overall dependence of read count ratio on diagnosis ($\Delta\text{AIC} = 2.0$, $p = 1.0$ for the random main effect ($1 \mid \text{Dx}$)) consistent with Figures 4 and 5. A related test for gene-specific effects of diagnosis, wherein the effect of Dx varies across the thirty genes, also yielded negative result ($\Delta\text{AIC} = 0.4$, $p = 0.21$ for the interaction term ($1 \mid \text{Dx} : \text{Gene}$)), which is again consistent with Figures 4 and 5. Together, these analyses indicate that diagnosis of SCZ or AFF does not have a substantial impact on the extent of allelic bias of imprinted genes in the DLPFC.

3.4 Gene-specific effects of age and ancestry

Fig. 5 shows that the read count ratio depends negatively on age for some imprinted genes (e.g. PEG3, ZNF331), depends positively for other genes (e.g. KCNK9, RP13-487P22.1), and is independent of age for the rest of imprinted genes (e.g. NDN, NLRP2). However, any apparent age effect may be indirect in the sense that it is mechanistically mediated by other explanatory variables to which age is associated with (Fig. S6).

To investigate the direct effect of age we turned to our best fitting mixed model once again, evaluating how significantly predictor terms associated with these variables improve the model's fit (Table 1). As for Dx we defined two terms for each variable, the term Age represents a fixed effect that is shared by all imprinted genes while the term (Age \mid Gene) symbolizes random, gene-specific, age effects. The shared effect was not supported by our criteria of model fit but the gene-specific effects received strong support at $\Delta\text{AIC} < -20$ and $p < 3 \times 10^{-5}$, which is consistent with the large gene-to-gene variation of age dependence suggested by Fig. 5.

The above result technically means a significantly greater than zero variance of the random

coefficients that mediate the gene-specific age effect. We complemented this with the posterior predicted values of those coefficients given the data and the estimated variance (Fig. S7 top middle). These predictions of isolated direct gene-specific age effects showed an overall agreement with the qualitative findings on mixed direct and indirect age dependence presented in Fig. 5 with some disagreements (e.g. for UBE3A) that likely reflect purely indirect dependence.

The same type of analysis on the effects of ancestry principal components and gender gave similar results. While the fixed effect, shared by all genes, of these variables was negligible, three of the random, gene-specific, effects received significant support. These three, ordered by decreasing statistical significance, are (Ancestry.1 | Gene), (Ancestry.3 | Gene) and (1 | Gender : Gene) (Table 1). The corresponding predicted random coefficients are presented in Fig. S7.

In summary age, ancestry, and to a lesser extent gender, are suggested by our model-based analysis to exert effect on allelic bias in a way that the direction and magnitude of the effect varies across genes.

4 Discussion

The number of imprinted genes in the brain has been controversial: early genome wide studies [8] estimated over a thousand but later the same authors and others [14, 6, 2] found that the statistical estimator was heavily biased and with more careful statistical analysis they discovered hundred or less imprinted genes in the brain. Our work reinforces the latter group of studies as we identified 30 imprinted genes in the DLPFC among the genes we could assess (about the third of all genes).

We have performed the most in-depth analysis up till now on the how imprinting depends on schizophrenia, as well as on age and other variables. This was made possible by (i) more study individuals than previous work [2] and well balanced case-control study groups, and (ii) powerful statistical inference based on a mixed model that captures much of the complex pattern of dependencies in genomic data. The modeled dependencies include those within and between technical and biological variables as well as the partial similarities among genes.

Although our approach gave strong support for dependence of imprinting on age and ancestry, no dependence on schizophrenia was detected either when we assumed that the dependence is the same for all imprinted genes or that it varies across genes. This might seem to suggest that imprinting in the DLPFC plays no significant role in schizophrenia and psychotic disorders contradicting the “imprinted brain” hypothesis [4]. Alternatively, imprinting does play a role in schizophrenia but only very strong perturbations of some imprinted genes increase the risk significantly, perturbations that are too rare to detect in even at our relatively large sample size. Additionally, the more subtle perturbations in our data might still have a significant effect when considered together with other genetic, epigenetic or environmental risk factors that were absent in our model. The complex genetic architecture of schizophrenia [18] makes these alternative explanations quite plausible.

We found that imprinting depends on ancestry in a gene specific manner but the type of dependence that is shared by all imprinted genes was not supported. This is expected because the studied ancestry variables must incorporate some of the cis expression QTLs in imprinted genes such that those eQTLs perturb allelic bias in a gene specific manner.

Our discovery that imprinting depends on age in later adulthood is rather intriguing. Although age dependence during embryonic development and childhood is both well-supported experimentally and well-understood, that during later adulthood has so far only been predicted [19] based on a hypothesis that links “genomic imprinting and the social brain” [10]. Previous genomics studies [2] were statistically underpowered to address this question in humans and the only experimental hints

were gained from young mice [14]. Although our age-related finding supports the “social brain” hypothesis, it leaves the possibility open that the observed age related changes indicate merely the loss of tight regulation of those genes after because they loose their functional significance in aging.

References

- [1] Yu Bai, Min Ni, Blerta Cooper, Yi Wei, and Wen Fury. Inference of high resolution HLA types using genome-wide RNA or DNA sequencing reads. *BMC Genomics*, 15(1):325, may 2014.
- [2] Yael Baran, Meena Subramaniam, Anne Biton, Taru Tukiainen, Emily K. Tsang, Manuel A. Rivas, Matti Pirinen, Maria Gutierrez-Arcelus, Kevin S. Smith, Kim R. Kukurba, Rui Zhang, Celeste Eng, Dara G. Torgerson, Cydney Urbanek, Jin Billy Li, Jose R. Rodriguez-Santana, Esteban G. Burchard, Max A. Seibold, Daniel G. MacArthur, Stephen B. Montgomery, Noah A. Zaitlen, and Tuuli Lappalainen. The landscape of genomic imprinting across diverse adult human tissues. *Genome Research*, 25(7), 2015.
- [3] Andrew F.G. Bourke. Kin Selection and the Evolutionary Theory of Aging. *Annual Review of Ecology, Evolution, and Systematics*, 38(1):103–128, dec 2007.
- [4] Bernard Crespi. Genomic imprinting in the development and evolution of psychotic spectrum conditions. *Biological reviews of the Cambridge Philosophical Society*, 83(4):441–93, nov 2008.
- [5] Bernard Crespi and Christopher Badcock. Psychosis and autism as diametrical disorders of the social brain. *The Behavioral and brain sciences*, 31(3):241–61; discussion 261–320, jun 2008.
- [6] Brian DeVeale, Derek van der Kooy, and Tomas Babak. Critical evaluation of imprinted gene expression by RNA-seq: A new perspective. *PLoS Genetics*, 8(3):e1002600, jan 2012.
- [7] Menachem Fromer, Panos Roussos, Solveig K Sieberts, Jessica S Johnson, David H Kavanagh, Thanneer M Perumal, Douglas M Ruderfer, Edwin C Oh, Aaron Topol, Hardik R Shah, Lambertus L Klei, Robin Kramer, Dalila Pinto, Zeynep H Gümü, A Ercument Cicek, Kristen K Dang, Andrew Browne, Cong Lu, Lu Xie, Ben Readhead, Eli A Stahl, Jianqiu Xiao, Mahsa Parvizi, Tymor Hamamsy, John F Fullard, Ying-Chih Wang, Milind C Mahajan, Jonathan M J Derry, Joel T Dudley, Scott E Hemby, Benjamin A Logsdon, Konrad Talbot, Towfique Raj, David A Bennett, Philip L De Jager, Jun Zhu, Bin Zhang, Patrick F Sullivan, Andrew Chess, Shaun M Purcell, Leslie A Shinobu, Lara M Mangravite, Hiroyoshi Toyoshiba, Raquel E Gur, Chang-Gyu Hahn, David A Lewis, Vahram Haroutunian, Mette A Peters, Barbara K Lipska, Joseph D Buxbaum, Eric E Schadt, Keisuke Hirai, Kathryn Roeder, Kristen J Brennand, Nicholas Katsanis, Enrico Domenici, Bernie Devlin, and Pamela Sklar. Gene expression elucidates functional impact of polygenic risk for schizophrenia. *Nature neuroscience*, sep 2016.
- [8] Christopher Gregg, Jiangwen Zhang, Brandon Weissbourd, Shujun Luo, Gary P Schroth, David Haig, and Catherine Dulac. High-resolution analysis of parent-of-origin allelic expression in the mouse brain. *Science (New York, N.Y.)*, 329(5992):643–8, aug 2010.
- [9] Andrés Ingason, George Kirov, Ina Giegling, Thomas Hansen, Anthony R Isles, Klaus D Jakobsen, Kari T Kristinsson, Louise le Roux, Omar Gustafsson, Nick Craddock, Hans-Jürgen Möller, Andrew McQuillin, Pierandrea Muglia, Sven Cichon, Marcella Rietschel, Roel A

- Ophoff, Srdjan Djurovic, Ole A Andreassen, Olli P H Pietiläinen, Leena Peltonen, Emma Dempster, David A Collier, David St Clair, Henrik B Rasmussen, Birte Y Glenthøj, Lambertus A Kiemeneij, Barbara Franke, Sarah Tosato, Chiara Bonetto, Evald Saemundsen, Stefán J Hreidarsson, GROUP Investigators, Markus M Nöthen, Hugh Gurling, Michael C O'Donovan, Michael J Owen, Engilbert Sigurdsson, Hannes Petursson, Hreinn Stefansson, Dan Rujescu, Kari Stefansson, and Thomas Werge. Maternally derived microduplications at 15q11-q13: implication of imprinted genes in psychotic illness. *The American journal of psychiatry*, 168(4):408–17, apr 2011.
- [10] Anthony R Isles, William Davies, and Lawrence S Wilkinson. Genomic imprinting and the social brain. *Philosophical transactions of the Royal Society of London. Series B, Biological sciences*, 361(1476):2229–37, dec 2006.
 - [11] Eric B Keverne. Genomic imprinting, action, and interaction of maternal and fetal genomes. *Proceedings of the National Academy of Sciences of the United States of America*, 112(22):6834–40, jun 2015.
 - [12] J F McDonald, M A Matzke, and A J Matzke. Host defenses to transposable elements and the evolution of genomic imprinting. *Cytogenetic and genome research*, 110(1-4):242–9, 2005.
 - [13] Gráinne I. McNamara and Anthony R. Isles. Dosage-sensitivity of imprinted genes expressed in the brain: 15q11q13 and neuropsychiatric illness. *Biochemical Society Transactions*, 41(3):721–726, jun 2013.
 - [14] Julio D Perez, Nimrod D Rubinstein, Daniel E Fernandez, Stephen W Santoro, Leigh A Needleman, Olivia Ho-Shing, John J Choi, Mariela Zirlinger, Shau-Kwaun Chen, Jun S Liu, and Catherine Dulac. Quantitative and functional interrogation of parent-of-origin allelic expression biases in the brain. *eLife*, 4:e07860, jan 2015.
 - [15] Jo Peters. The role of genomic imprinting in biology and disease: an expanding view. *Nature reviews. Genetics*, 15(8):517–30, aug 2014.
 - [16] Robert N Plasschaert and Marisa S Bartolomei. Genomic imprinting in development, growth, behavior and stem cells. *Development (Cambridge, England)*, 141(9):1805–13, may 2014.
 - [17] M. B. Renfree, S. Suzuki, and T. Kaneko-Ishino. The origin and evolution of genomic imprinting and viviparity in mammals. *Philosophical Transactions of the Royal Society B: Biological Sciences*, 368(1609):20120151–20120151, nov 2012.
 - [18] Patrick F Sullivan, Mark J Daly, and Michael O'Donovan. Genetic architectures of psychiatric disorders: the emerging picture and its implications. *Nature Reviews Genetics*, 13(8):537–551, aug 2012.
 - [19] Francisco Ubeda and Andy Gardner. A model for genomic imprinting in the social brain: elders. *Evolution; international journal of organic evolution*, 66(5):1567–81, may 2012.
 - [20] Jon F Wilkins and David Haig. What good is genomic imprinting: the function of parent-specific gene expression. *Nature reviews. Genetics*, 4(5):359–68, may 2003.

- [21] X Zheng, J Shen, C Cox, J C Wakefield, M G Ehm, M R Nelson, and B S Weir. HIBAG—HLA genotype imputation with attribute bagging. *The Pharmacogenomics Journal*, 14(2):192–200, apr 2014.
- [22] Lillian M Zwemer, Alexander Zak, Benjamin R Thompson, Andrew Kirby, Mark J Daly, Andrew Chess, and Alexander A Gimelbrant. Autosomal monoallelic expression in the mouse. *Genome Biology*, 13(2):R10, feb 2012.

predictor term	interpretation	ΔAIC	p-value
(1 Gene)	variability among genes	-126.8	8.5×10^{-28}
(1 Dx)	variability among Control, SCZ, AFF	2.0	1.0
(1 Dx : Gene)	Gene specific variability among Ctrl, SCZ, AFF	0.4	0.21
Age	effect of Age	1.3	0.39
(Age Gene)	Gene specific effect of Age	-18.9	2.5×10^{-5}
Ancestry.1	effect of Ancestry.1	0.6	0.24
(Ancestry.1 Gene)	Gene specific effect of Ancestry.1	-71.2	4.6×10^{-16}
Ancestry.3	effect of Ancestry.3	1.6	0.54
(Ancestry.3 Gene)	Gene specific effect of Ancestry.3	-17.9	3.8×10^{-5}
(1 Gender)	difference between Male and Female	2.0	1.0
(1 Gender : Gene)	Gene specific difference between M and F	-5.7	5.5×10^{-3}

Table 1: Selected biological terms in the predictor of a mixed model and their impact on model fit. The smaller (more negative) ΔAIC , and the smaller the p-value (χ^2 -test), the more likely that the term has non-zero effect on the read count ratio. For further discussion on interpretation and mathematical properties of terms see Section 2.4.2.

5 Figures, Tables and Supplementary Material

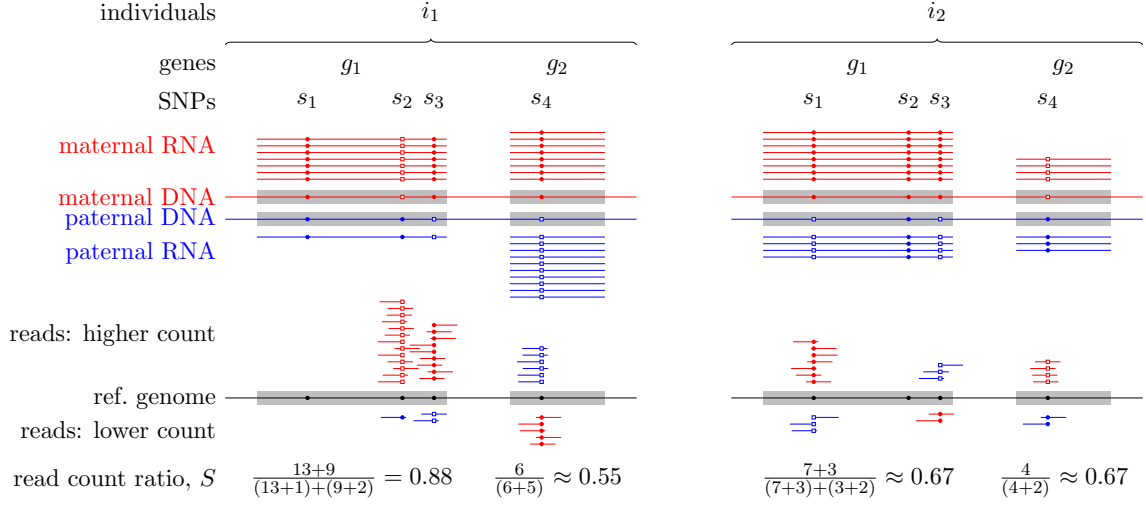


Figure 1: Quantifying allelic bias of expression in human individuals using the RNA-seq read count ratio statistic S_{ig} . The strength of bias towards the expression of the maternal (red) or paternal (blue) allele of a given gene g in individual i is gauged with the count of RNA-seq reads carrying the reference allele (small closed circles) and the count of reads carrying an alternative allele (open squares) at all SNPs for which the individual is heterozygous. The allele with the higher read count tends to match the allele with the higher expression but measurement errors may occasionally revert this tendency as seen for SNP s_3 in gene g_1 in individual i_2 .

explanatory variable	levels
Age	
Institution	[MSSM], Penn, Pitt
Gender	[Female], Male
PMI	
Dx	[Control], SCZ, AFF
RIN	
RNA_batch	[A], B, C, D, E, F, G, H, 0
Ancestry.1	
\vdots	
Ancestry.5	

Table S1: *Left column:* explanatory variables of read count ratio. *Right column:* levels of each factor-valued (i.e. categorical) variable. Square brackets [...] surround the baseline level against which other levels are contrasted. *Abbreviations:* PMI: post-mortem interval; Dx: disease status; AFF: affective spectrum disorder; SCZ: schizophrenia; RIN: RNA integrity number; Ancestry. k : the k -th eigenvalue from the decomposition of genotypes indicating population structure.

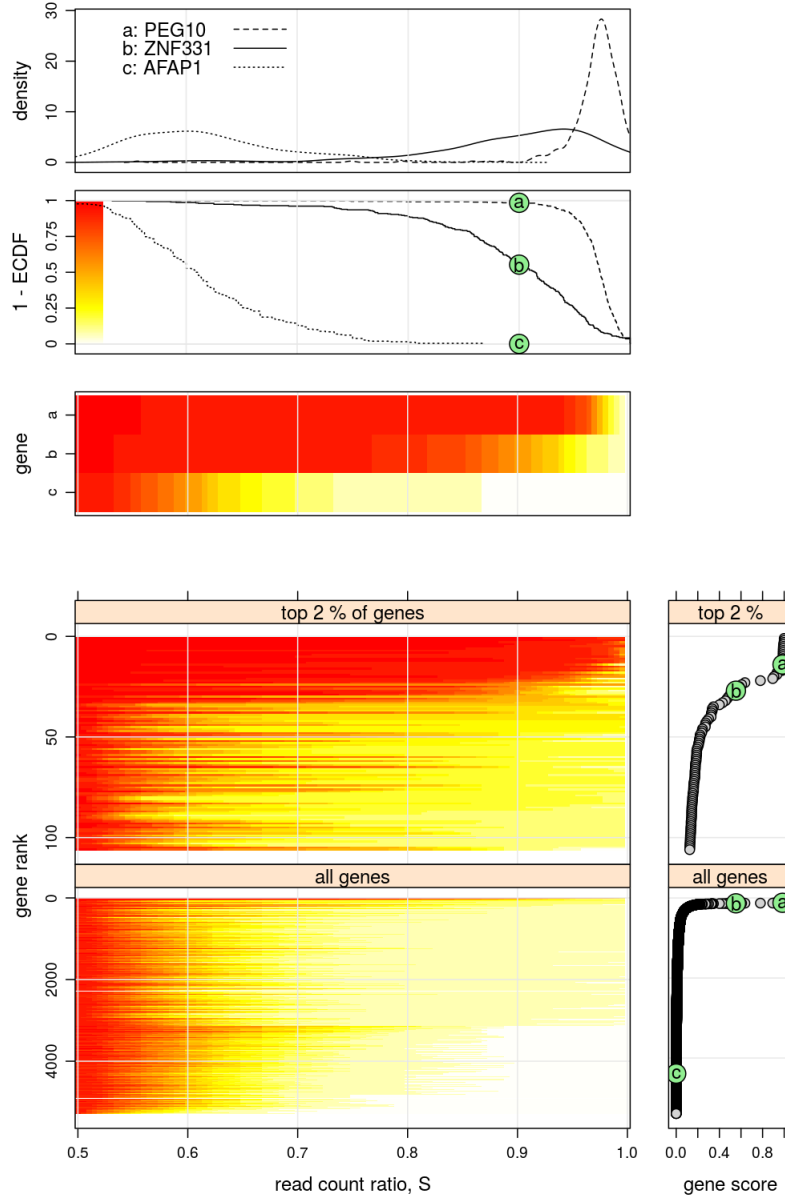


Figure 2: Using the read count ratio statistic S to report on variation of allelic bias across individuals and genes. *Upper half*, from top to bottom: (1) kernel density estimate; (2) the graph of the survival function $1 - \text{ECDF}$, where ECDF means empirical cumulative distribution function; note color scale for heat map and green filled circles marking genes' score; (3) the heat map representation of the survival function. *Lower half*, main panels: heat map of the survival function for all 5307 analyzed genes ranked according to their score; right side panels: gene score.

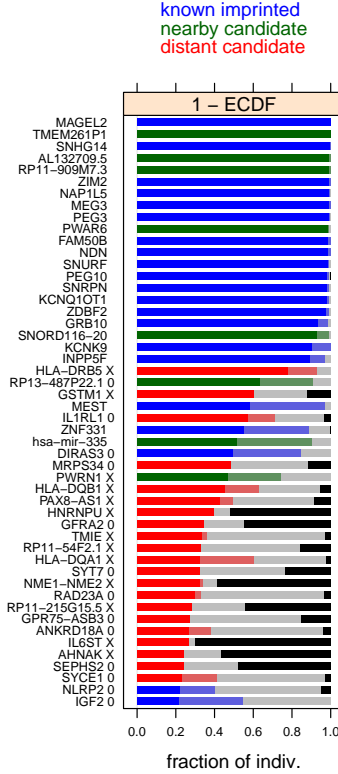


Figure 3: The top 50 genes ranked by the gene score. The score of gene g is $1 - \text{ECDF}_g(0.9)$, the fraction of individuals i for which $S_{ig} > 0.9$ and is indicated by the length of dark blue, dark green or dark red bars. Note that the same ranking and score is shown in the bottom half of Fig. 2. The right border of the light blue, light green and light red bars is at $1 - \text{ECDF}_g(0.8)$. The length of the black bars indicates the fraction of individuals passing the test of nearly unbiased expression (Eq. 2). “X” characters next to gene names indicate reference allele bias, while “0” indicate that reference allele bias could not be determined due to small amount of data.

model family	abbrev.	response var.
unweighted normal linear	unlm	S, Q , or R
weighted normal linear	wnlm	S, Q , or R
logistic	logi	S
logistic, $\frac{1}{2} \times$ down-scaled link fun.	logi2	S

Table S2: Fitted regression model families, in which the response variable is the read count ratio with or without some transformation: S —untransformed, Q —quasi-log-transformed, and R —rank-transformed read count ratio. Diagnostic plots (Fig. S2, S3) and monitoring convergence suggested that the unlm. Q combination allows the best fit for several linear predictors tested.

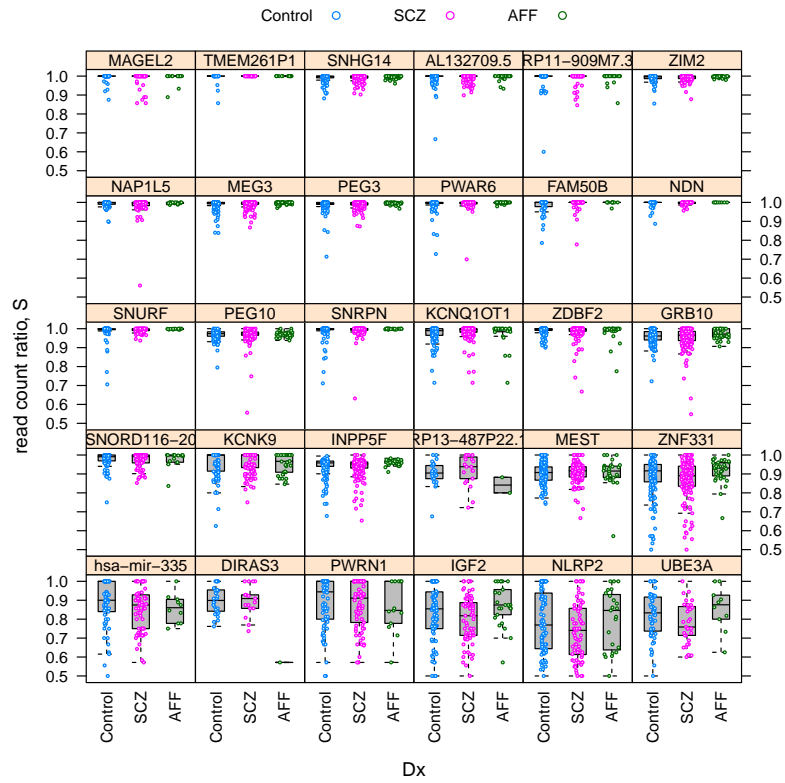


Figure 4: Distribution of read count ratio for control, schizophrenic (SCZ), and affective spectrum (AFF) individuals within each gene that has been considered as imprinted in the DLPFC brain area in this study.

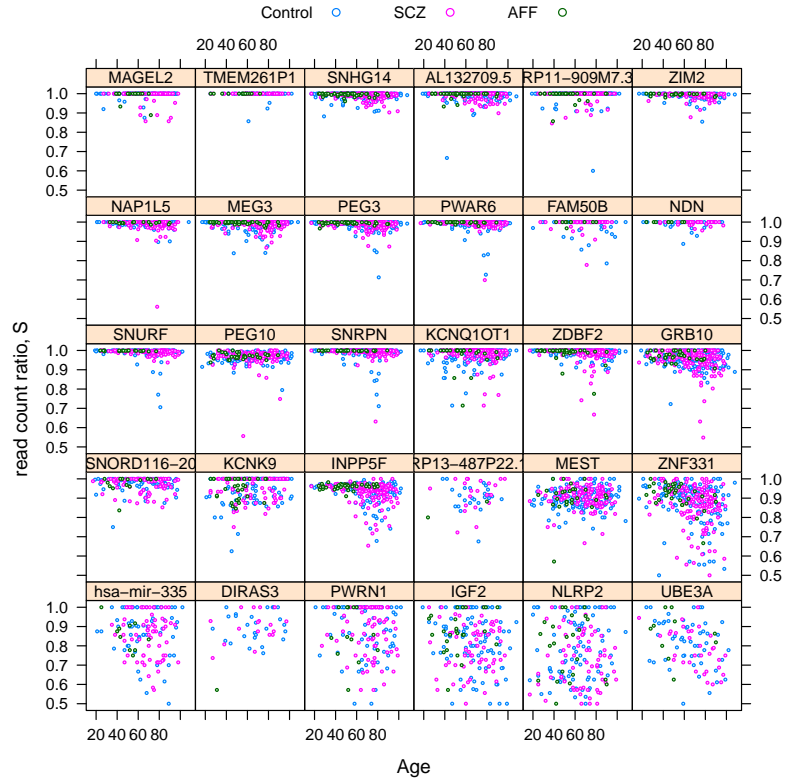


Figure 5: Variation of read count ratio with age.

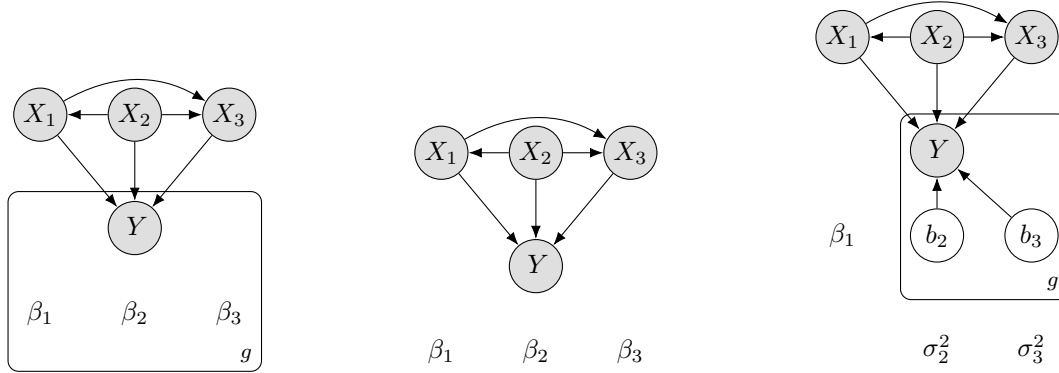


Figure S1: General dependency structures in two fixed effects regression models (*left, middle*) and a mixed effects model (*right*). In all three cases the regression coefficients $\beta_{1g}, \dots, \beta_{3g}$ or $\beta_{1g}, b_{2g}, b_{3g}$ mediate, for a given gene g , probabilistic dependencies (arrows) between the response variable Y_g (read count ratio for g) and the corresponding explanatory variables X_1, \dots, X_3 . For simplicity but without loss of generality only 3 explanatory variables are depicted. The model frameworks differ in how the coefficients relate to each other for a given explanatory variable (or a given j). *Left*: there is no connection among $\beta_{jg_1}, \beta_{jg_2}, \dots$ which means that the way Y_g , the read count ratio for gene g depends on variable X_j is completely separate from how the read count ratio for any other gene g' (i.e. $Y_{g'}$) depends on it. Consequently no information may be shared among gene-specific models. *Middle*: In this case $\beta_{jg_1} = \beta_{jg_2} = \dots \equiv \beta_j$ so that all genes are identical with respect to how their read count ratio depends the explanatory variables. Thus genes share all information in the data in the sense that the model forces them to be identical. *Right*: Hierarchical mixed effects model where certain dependencies (β_1) are shared among genes while others ($\{b_{2g}\}_g, \{b_{3g}\}_g$) vary across genes. The variation is controlled by the variance parameters σ_j^2 . In this example there is a single set $\{b_{2g}\}_g$ of random coefficients for X_2 —and a similar set for X_3 —, which are random intercepts. In general, however, one or more set of random slope coefficients may also be present. Given the estimates $\hat{\sigma}_j^2$ and the data the gene-specific random coefficients b_{jg} can be predicted. Among the three only this model framework allows information sharing among genes in a flexible way.

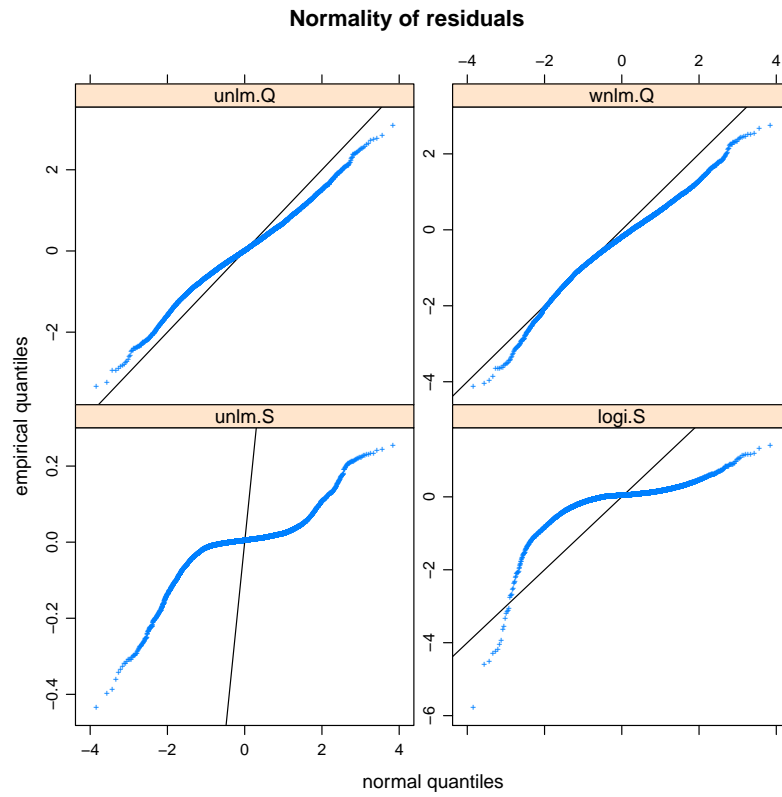


Figure S2: Checking the fit of various model families: analysis of the normality of residuals.

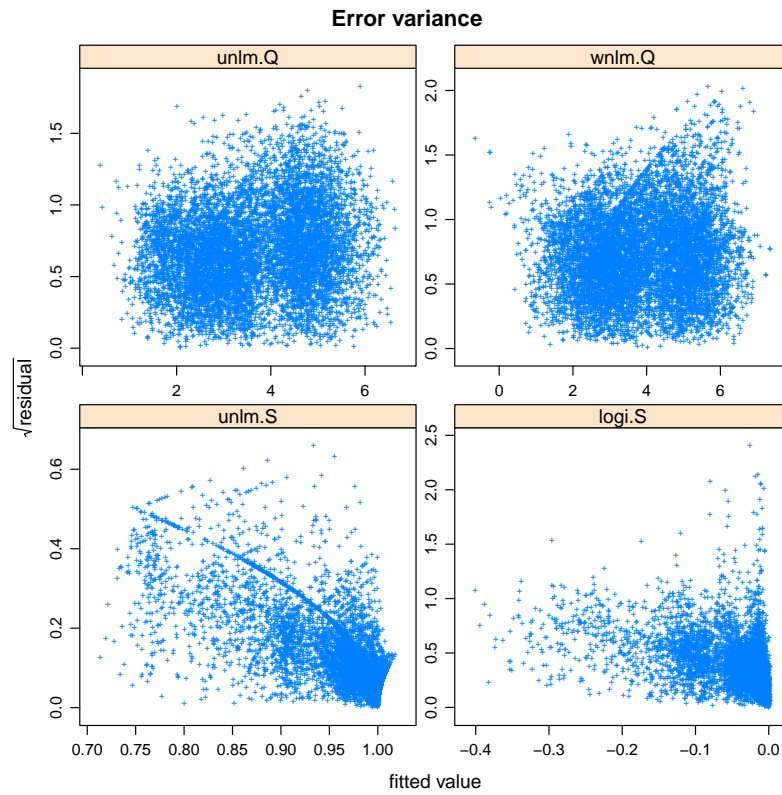


Figure S3: Checking the fit of various model families: analysis of homoscedasticity.

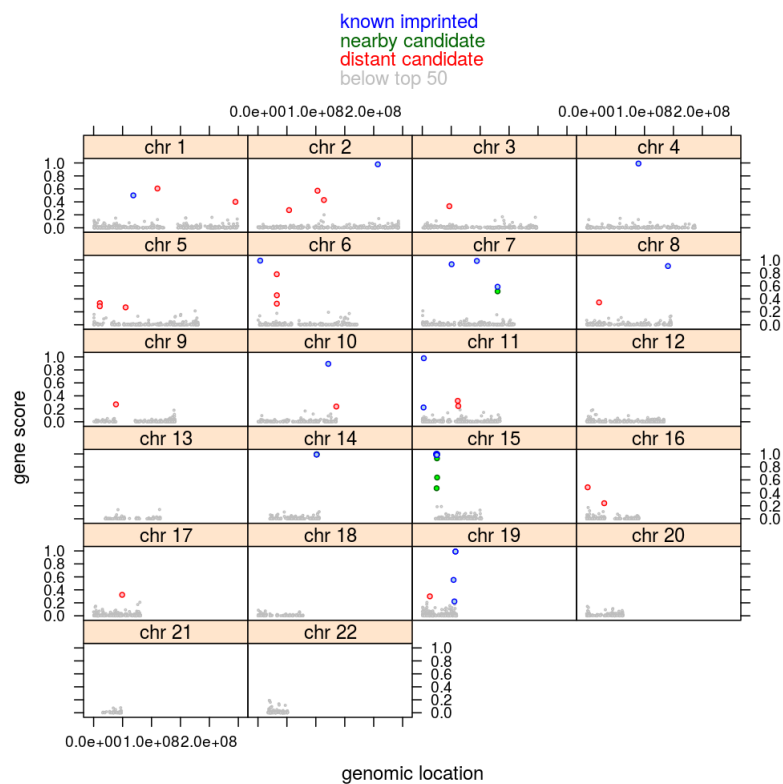


Figure S4: Clustering of top-scoring genes in the context of human DLPFC around genomic locations that had been previously described as imprinted gene clusters in other contexts.

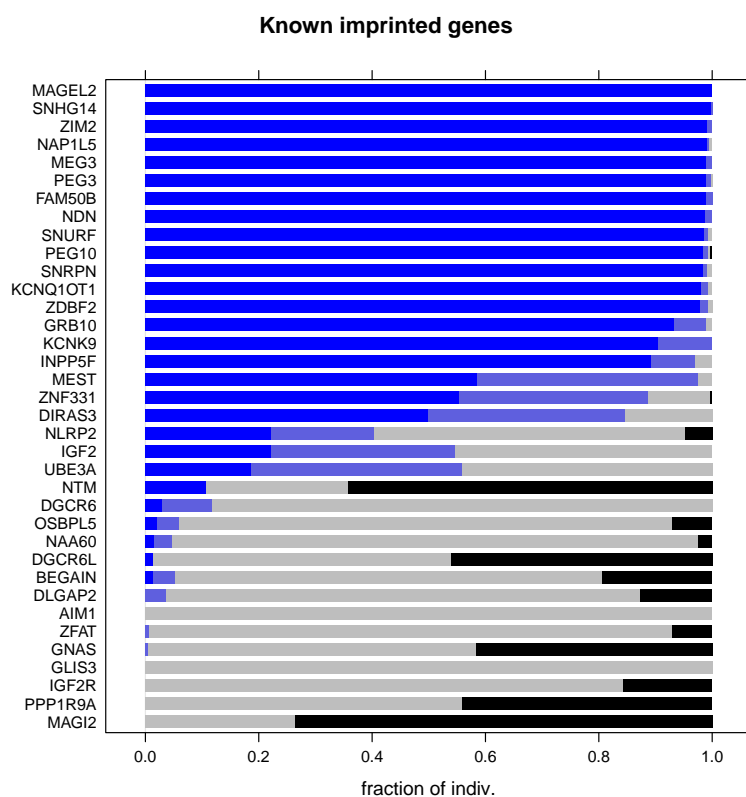


Figure S5: Known imprinted genes ranked by the gene score (dark blue bars). “Known imprinted” refers to prior studies on imprinting in the context of any tissue and developmental stage. The length of the black bars indicates the fraction of individuals passing the test of nearly unbiased expression.

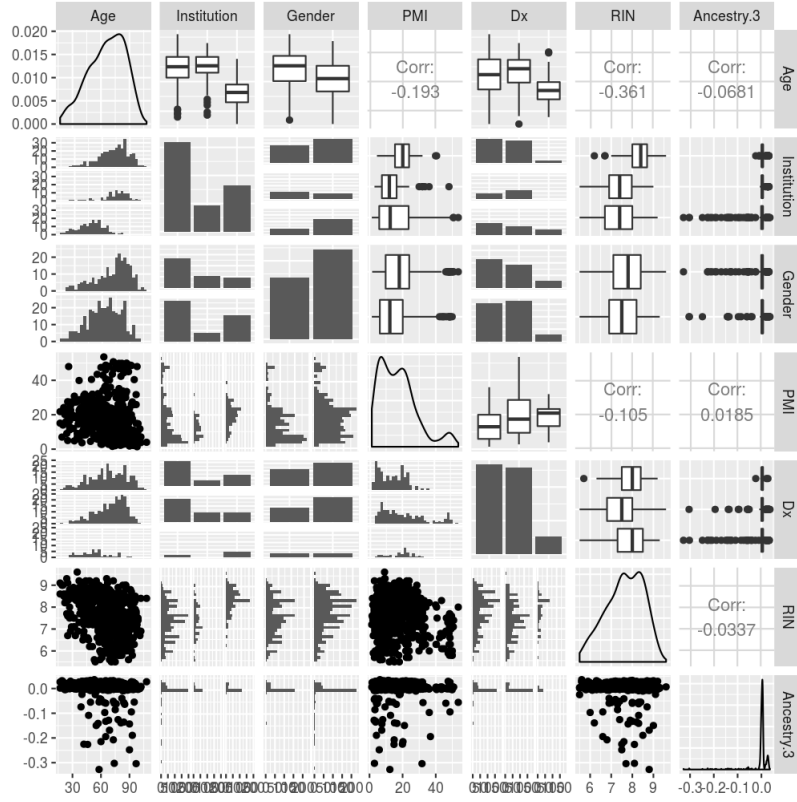


Figure S6: Distribution and inter-dependence of explanatory variables. The diagonal graphs of the plot-matrix show the marginal distribution of six variables (Age, Institution,...) while the off-diagonal graphs show pairwise joint distributions. For instance, the upper left graph shows that, in the whole cohort, individuals' Age ranges between ca. 15 and 105 years and most individuals around 75 years; the bottom and right neighbor of this graph both show (albeit in different representation) the joint distribution of Age and Institution, from which can be seen that individuals from Pittsburg tended to be younger than those from the two other institutions.

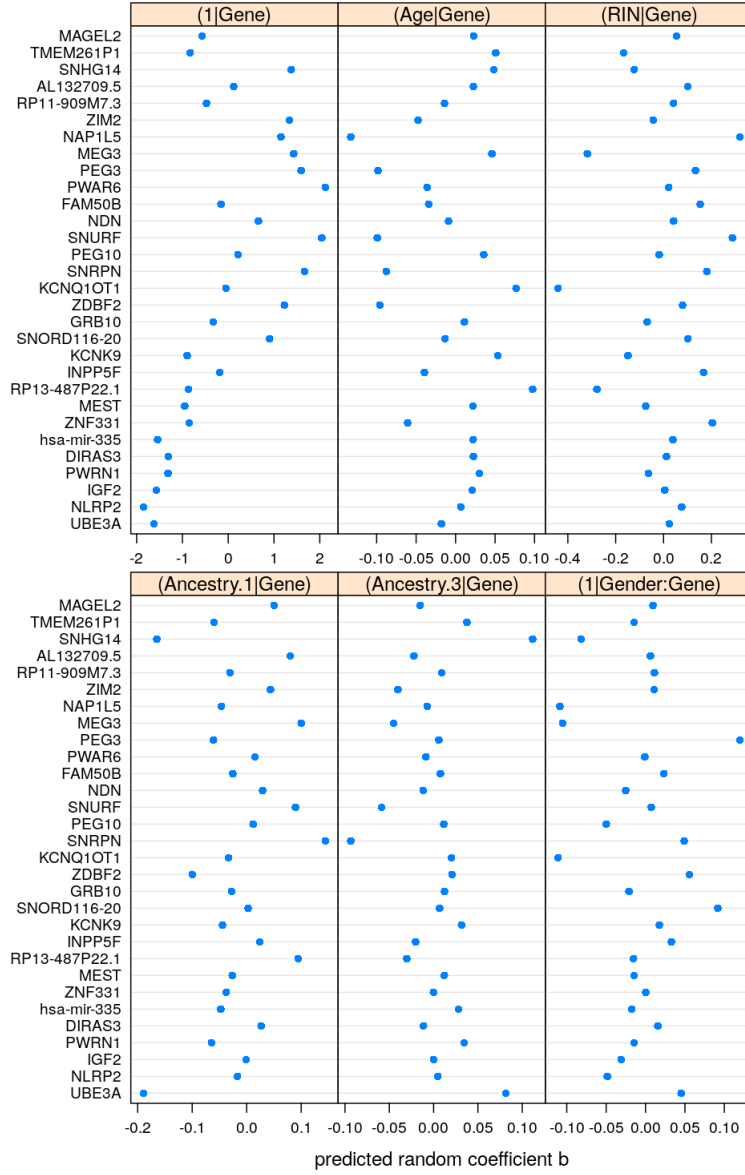


Figure S7: Predicted random coefficients b_{gj} for gene g (y -axis) and random effect j (panel headers). Positive and negative coefficient indicates direct positive and negative dependence of the given gene's read count ratio on age, respectively, while zero coefficient suggests independence of age. Compare with Fig. 5.